HHS Public Access

Author manuscript

Nat Microbiol. Author manuscript; available in PMC 2017 July 30.

Published in final edited form as:

Nat Microbiol. ; 2: 16272. doi:10.1038/nmicrobiol.2016.272.

Structural basis for antibody cross-neutralization of respiratory syncytial virus and human metapneumovirus

Xiaolin Wen[1], **Jarrod J. Mousa**[2], **John T. Bates**[2], **Robert A. Lamb**[3,4], **James E. Crowe Jr.**[2,5,6], and **Theodore S. Jardetzky**[1]

[1]Department of Structural Biology, Stanford University School of Medicine, Stanford California 94305

[2]Vanderbilt Vaccine Center, Vanderbilt University School of Medicine, Nashville, TN, USA

[3]Howard Hughes Medical Institute, Northwestern University, Evanston, IL 60208-3500

[4]Department of Molecular Biosciences, Northwestern University, Evanston, IL 60208-3500

[5]Department of Pediatrics, Vanderbilt University School of Medicine, Nashville, TN, USA

[6]Department of Pathology, Microbiology and Immunology, Vanderbilt University School of Medicine, Nashville, TN, USA

Respiratory syncytial virus (RSV) and human metapneumovirus (HMPV) are two closely related viruses that cause bronchiolitis and pneumonia in infants and the elderly[1], with a significant health burden[2–6]. There are no licensed vaccines or small molecule antiviral treatments specific to these two viruses currently. While a humanized murine monoclonal antibody (palivizumab) is approved to treat high risk infants for RSV infection[7,8], other treatments, as well as vaccines, for both viruses are still in development. Recent epidemiological modeling suggests that cross-immunity between RSV, HMPV and human parainfluenzaviruses may contribute to their periodic outbreaks[9], suggesting that a deeper understanding of host immunity to these viruses may lead to enhanced strategies for their control. Cross-reactive neutralizing antibodies to the RSV and HMPV fusion (F) proteins have been identified[10,11]. Here we examine the structural basis for cross-reactive antibody binding to RSV and HMPV F protein by two related, independently isolated antibodies, MPE8 and 25P13. We solved the structure of the MPE8 antibody bound to RSV F and identified the 25P13 antibody from an independent blood donor. Our results indicate that both antibodies use germline residues to interact with a conserved surface on F that could guide the emergence of cross-reactivity. The induction of similar cross-reactive neutralizing

Correspondence and request for materials should be addressed to TSJ (tjardetz@stanford.edu).

Data availability: The DS-CAV1:MPE8 complex crystal structure and reflection data have been deposited in the Protein Data Bank under the accession code 5U68. Other data supporting the findings of this study are available on request.

Author contributions: Conceived and designed the experiments: XW, JJW, JTB, RAL, JEC & TSJ; Performed the experiments: XW, JJW, JTB; Analyzed the data: XW, JJW, JTB, RAL, JEC & TSJ; Contributed reagents/materials/analysis tools: XW, JJW, JTB; Wrote and edited the manuscript: XW, JJW, JTB, RAL, JEC & TSJ.

Competing interests: One of the authors (J.E.C) declares a competing interest. The remaining authors declare no competing interests.

antibodies using structural vaccinology approaches, could enhance intrinsic cross-immunity to these paramyxoviruses and approaches to controlling recurring outbreaks.

The RSV/HMPV F protein is a class I viral fusion protein that refolds to drive membrane fusion and virus entry[12–18], and it is the major target of the neutralizing antibody response. MPE8 was isolated from human B cells based on its ability to cross-neutralize a panel of RSV and HMPV strains[10]. We determined the crystal structure of an MPE8 variant in complex with a stabilized prefusion RSV F trimer (DS-CAV1)[19–22]. We generated single chain Fv (scFv) constructs for MPE8 and predicted unmutated common ancestor (UCA) variants that have retain RSV F binding and neutralization[10] (Supplementary Figure 1,2). Complexes of MPE8 with DS-CAV1[22] were prepared by co-transfection of 293-6E cells, and purified using affinity and gel filtration chromatography (Supplementary Figure 3). Optimized crystals of DS-CAV1 with the MPE8 scFv variant consisting of the predicted UCA heavy chain variable domain (VH_{gl}) and the fully mature light chain variable domain (VL_{sm}) were obtained and the structure was solved by molecular replacement (Fig. 1, Methods and Supplementary Table 1).

MPE8 binds an epitope near the midsection of the RSV F ectodomain (Fig. 1a,c), consistent with previous mapping studies[10]. The interface buries ~1,100 $Å^2$ of surface on each of the proteins (2,200 $Å^2$ total). The three scFvs are positioned with VH and VL domains aligned nearly perpendicular to the long axis of the F trimer and parallel to the predicted plane of the viral membrane. When viewed along the three-fold axis of the trimer, the MPE8 V domains radiate horizontally outwards from three apices of the F subunits, engaging the widest section of the F head domain (Fig. 1b,d). MPE8 binds preferentially to prefusion F. Its conformational specificity has three apparent structural determinants. First, MPE8 engages RSV F residues located spanning two neighboring subunits of the trimer (Fig. 1c,d), defining an intersubunit epitope present only in the prefusion conformation. Second, MPE8 contacts two β-strands of the prefusion heptad repeat A (HRA), which refold into a long helix and move away from the MPE8 interface in the postfusion form[14,17] (Supplementary Figure 4a,b). Third, docking of MPE8 onto the postfusion F structure indicates that steric clashes between F DII and the MPE8 VL domain could interfere with binding (Supplementary Figure 4c,d).

Most of the MPE8 epitope lies within 1 subunit of the F trimer, involving residues in DI and DIII, with a smaller contact area in DII of the neighboring subunit (Fig. 2a). The DIII contacts overlap the helix-turn-helix motif of the palivizumab/motavizumab site A epitope (Fig. 2a,b). The VH domain lies distal to the F trimer interface, primarily contacting the F surface below and to one edge of site A (Fig. 2a–c). The HCDR3 loop extends underneath the site A motif in DIII to insert its tip into a pocket formed at the intersubunit interface (Fig. 2b,c), with residues Y100 and N100A forming contacts dependent on the prefusion F conformation. HCDR3 residues (100B–100G) interact with the turn residues within site A (Fig. 2b). HCDR2 also forms interactions with the second helix of site A and with residues in DI, while HCDR1 contacts F below site A in DI (Fig. 2c). RSV F mutations that have been shown previously to affect MPE8 binding also map to the structural interface (Supplementary Figure 5). The mutation of D310A would disrupt interactions with HCDR2

and many of these previously identified mutations line the groove along which HCDR3 extends (L305R, G307R, R49D and T50A).

The VL domain is positioned near the trimer interface with LCDR2 contacting DII of the adjacent subunit (Fig. 2c). LCDR2 interactions across the trimer, together with HCDR3, would contribute to preferential binding to prefusion F. LCDR1 and LCDR3 interact with the first helix of site A (Fig. 2). LCDR1 also contacts two beta strands of the DIII HRA motif (F residues 178, 180 and 184–187), present only in the prefusion conformation (Supplementary Figure 4). The MPE8 paratope is a relatively flat surface comprised of the 6 CDR loops, with the heavy chain HCDR3 wrapping across the front of the VH domains and covering LCDR2 (Fig. 2d). HCDR1, HCDR2 and HCDR3 form an L-shaped surface that defines the majority of the MPE8 binding surface, with HCDR3 inserting into the F intersubunit groove.

The MPE8 epitope is only partially conserved in HMPV (Fig. 3a and Supplementary Table 2). HCDR1 and HCDR2 anchor the antibody to the largest contiguous surface of conserved residues (Fig. 3a). HCDR3 extends along a narrower conserved segment to contact additional, more fragmented patches of surface residue conservation. The light chain, particularly LCDR1, also contacts smaller, more isolated islands of conserved residues (Fig. 3a). MPE8 crossreactivity appears to be achieved by the formation of a large interface with a mosaic patchwork of conservation rather than by a narrow focus on a single conserved site.

The predicted MPE8 UCA selectively neutralizes RSV, but not HMPV[10], indicating that cross-reactivity emerges as a result of somatic hypermutation that broadens its reactivity to HMPV. Fourteen residues in MPE8, 9 in VH and 5 in VL, are mutated in mature MPE8. VL residues play a major role in HMPV cross-reactivity[10]. In the MPE8 structure, three of the five VL residues (D50, N52 and R93) are located in or near the RSV F interface (Fig. 3b,c). For VH, only three of the nine somatic mutations are within the RSV interface (residues S52A, Y58 and N100A in VH_{gl}; Fig. 3b,c). VL D50 is a major determinant of cross-reactivity to HMPV F[10]. Mutation of D50 to glycine, representing a reversion to the UCA, ablates HMPV F binding. D50 is located behind HCDR3 and does not directly contact F, but forms a hydrogen bond to HCDR3 residue T98 (Fig. 3d). D50 may therefore indirectly stabilize an HCDR3 conformation that can bind both RSV and HMPV F, similar to somatic mutations observed in other antibodies. Mutation of VL R93S in LCDR3 reduces MPE8 binding to HMPV B strains[10]. R93 lies above antigenic site A and forms a hydrogen bond with the main chain of RSV F residue 263 (Fig. 3b,c). To a lesser extent, somatically mutated residues in VH have also been shown to influence MPE8 cross-reactivity[10]. The structure indicates that these effects are likely due to VH residues Y58 and N100A in HCDR2 and HCDR3, respectively. Y58, the predicted germline residue, forms contacts to RSV F D310, an F residue important for MPE8 binding. N100A is at the tip of HCDR3 and is mutated to serine in the mature MPE8 sequence (Fig. 2b,c).

To further explore the diversity of cross-reactive antibodies to RSV and HMPV, we identified a novel antibody (25P13) from a blood donor that also binds and neutralizes both RSV and HMPV F (Fig. 4a). 25P13 binding is stronger to a chimeric HMPV F protein with a grafted RSV F site A (RPM-1)[23] than it is to wt HMPV F, providing a preliminary

mapping of its epitope (Fig. 4a). Cross-competition assays with a panel of RSV specific antibodies show that 25P13 competes with MPE8, as well as motavizumab and palivizumab (Fig. 4b), while partially competing with 101F and 54G10 antibodies. The similar cross-competition pattern for MPE8 and 25P13 indicates that both antibodies overlap antigenic sites site A and IV. However, in contrast to MPE8, 25P13 binds more readily to postfusion RSV F (Fig. 4c).

We sequenced the 25P13 heavy and light chain variable regions (Fig. 4d, Supplementary Figure 6). 25P13 uses the same VH gene segment (3-21*01) as MPE8 and a closely related or identical V_L segment (Fig. 4d). Sequences of the HCDR and LCDR loops show significant homology. In particular, residues in MPE8 HCDR1 and HCDR2 are >80% conserved, indicating that 25P13 could engage the same conserved surface patch of residues on F similar to MPE8 (Fig. 3a). Indeed, 25P13 and MPE8 both lose binding to RSV F DS-CAV1 with the D310A mutation (Fig. 4e and Supplementary Figure 5). LCDR3 is also well conserved (7 out of 10 residues), including two key residues (Y107 and R93) that are buried in the MPE8 complex with RSV F. HCDR3 exhibits the largest differences (~50% identity) and is shorter by two residues, indicating that the 25P13 HCDR3 would not insert as deeply into the intersubunit crevice in F and may not engage two subunits of F as observed for MPE8 (Fig. 2). A G307R mutation was previously shown to disrupt MPE8 binding[10]. This mutation significantly reduces but does not eliminate 25P13 binding, consistent with interaction differences of its shorter HCDR3 loop (Fig. 4e and Supplementary Figure 5). Together, these data indicate that related cross-reactive neutralizing antibodies can be readily identified, which utilize germline HCDR1 and HCDR2 sequences to anchor interactions with F through a conserved surface determinant present in RSV and HMPV F proteins.

The MPE8 epitope is distinct from other structurally characterized anti-F antibodies (Supplementary Figure 7). D25[14] and AM14[24] are two neutralizing antibodies specific for the prefusion F conformation, while motavizumab can bind both pre and post-fusion RSV F. D25 binds an epitope in the top of DIII that does not have any overlap with MPE8[14]. Low-resolution structures of AM14 and motavizumab with RSV F have been determined[24] and binding of both of these antibodies would be sterically blocked by MPE8. The epitopes of AM14 and motavizumab partially overlap that of MPE8. However, only MPE8 engages the larger patch of conserved residues lying below the site A epitope that provides its nascent cross-reactivity (Fig. 3a).

Broadly neutralizing antibodies to HIV Env and to influenza virus HA have been shown in several cases to involve a focusing of the antibody interaction on highly conserved elements of an indispensible functional site[25–28]. MPE8 and 25P13 appear to achieve their cross-reactivity through an anchoring interaction mediated by germline HCDR1 & HCDR2 loops with a conserved F surface within DI, while fine tuning interactions across a patchwork of conserved and non-conserved epitope residues. Specific recognition of the prefusion F conformation through this cross-reactive site is not required for neutralization, as shown by our observations with 25P13, although the conformational specificity of MPE8 could contribute to its greater potency of neutralization. Other potentially cross-reactive antibodies to RSV and HMPV, which bear the same VH domain as MPE8 and 25P13, may be present

as nascent variants within the antibody repertoire, providing an attractive target for structure-based vaccine design.

Materials and Methods

Expression and purification of proteins

The gene encoding the stabilized prefusion DS-CAV1 RSV F trimer[22] was synthesized (GeneWiz) and cloned into the PTT5 expression vector (National Research Council (NRC), Canada) with a T4-fibritin trimerization domain in-frame with the heptad repeat of the C-terminal HRB, and with Thrombin cleavage site. The wt MPE8 single chain Fv (scFv) gene was synthesized by Life Technologies as a GeneArt® Strings™ DNA Fragment, was cloned into the pCEP4 expression vector (Invitrogen) and contains a C-terminal TEV cleavage site and His6 tag. The RSV F and scFv expression plasmids were prepared using the Plasmid Mega Kit (Qiagen) and transfected into suspension 293-6E cells (NRC) at a density of 1.8 to 2.0 million cells/mL using 25-kDa linear polyethylenimine (Polysciences), (PEI) following 293-6E cell protocols. Supernatants were harvested five days post-transfection by centrifugation (20 min at 8,000 × *g* at room temperature), filtered through 0.45 μm filters and dialyzed against 200 mM NaCl, 50 mM Na2HPO4 pH 7.4. The RSV F protein was purified by Co^{2+} affinity chromatography (TALON Resin, BD Biosciences) and size exclusion chromatography using a Superdex-200 column equilibrated in 25 mM sodium phosphate, pH 7.4, and 100 mM NaCl, 100 mM imidazole. The purified protein was concentrated with Amicon Ultra centrifugal filters with a 10 kD molecular weight cut-off (Millipore). RSV F mutants L305R, G307R and D310A were prepared from the DS-CAV1 RSV F construct (Biozilla –Mutagenesis). Additional MPE8 variants were synthesized and cloned into the PTT5 expression vector corresponding to hGL-lGL, hGL-lSM, hSM-lSM D50G and hGL-lGL G56D. The MPE8 mutant proteins were expressed similarly to wild-type MPE8 in 293-6E cells, with supernatants harvested five days post-transfection. The MPE8 proteins were purified by Co^{2+} affinity chromatography and size exclusion chromatography and concentrated as with wild-type MPE8.

RSV F DS-CAV1 mutants L305R, G307R, and D310A were expressed in expiCHO cells following the manufacturer's protocol, harvested after six days, and purified by HiTrap TALON crude columns (GE Healthcare). cDNAs encoding the published variable gene sequences encoding the mAbs motavizumab, 101F, and D25 were synthesized (Genscript), and heavy and light chain sequences were cloned into vectors encoding human IgG1 and lambda or kappa light chain constant regions, respectively. Plasmids encoding the heavy and light chains of mAb 54G10 were a gift from Dr. Dennis Burton (Scripps Research Institute). Mab 131-2a protein was obtained from Sigma (MAB8599). Commercial preparations of palivizumab (Medimmune) were obtained from the pharmacy at Vanderbilt University Medical Center. Recombinant mAbs were expressed in HEK293F cells for 5 days following the manufacturer's protocol and purified by HiTrap MabSelectSure columns (GE Healthcare).

Crystallization and structure determination of the MPE8:RSV F complex

Complexes of MPE8 scFvs with the DS-CAV1 RSV F variant were prepared by co-transfection of 293 6E cells, followed by purification using Co^{2+} affinity chromatography and gel filtration chromatography. Complexes of MPE8 with the DS-CAV1 RSV F were observed using size exclusion chromatography with a Superdex-200 column (Supplementary Figure 3) and verified by SDS–PAGE. Complexes were dialyzed into 25 mM Tris-HCl and 125 mM NaCl pH 7.0 and concentrated to 6–8 mg/mL. Crystals were grown from hanging drops with a well solution containing 0.1M Potassium Nitrate, 0.1M Citrate Phosphate pH 4.2, 1% Tacsimate pH 7.0, 14% PEG 6000. Crystals appeared after 3–10 days.

Native crystals were transferred to a cryoprotectant solution of 0.1M Potassium Nitrate, 0.1M Citrate Phosphate pH 4.2, 1% Tacsimate pH 7.0, 14% PEG 6000 and 15% glycerol, followed by flash cooling in liquid nitrogen. Data were collected at LS-CAT 21-ID-F beamline at the Advanced Photon Source (APS) - Argonne National Laboratory. Crystals belong to space group P3121 and exhibited significant diffraction anisotropy. The native data were initially processed to 3.1 Å with XDS and then submitted to the Diffraction Anisotropy Server, which truncated the data to 3.1 Å along the c* axis and 3.6 Å along the a*/b* axes (Supplementary Table 1).

Molecular replacement searches were conducted with the program PHASER[29] using the CCP4 suite of programs[30]. The PCSK9 Fab model (3H42) and prefusion RSV F model (4JHW) yielded clear molecular replacement solutions. Initial refinement provided an R_{free} of 39.91% and R work of 41.14%. Automated model building to improve early models was performed using Phenix AutoBuild[31]. The complex structure was refined using Phenix Refine[32], followed by manual rebuilding with the program COOT[33]. The F model starts with residue 25 and ends with residue 509 (of 562 in the ectodomain construct). The Fv VH model starts with residue E1 and ends with residue S113, the Fv VL model starts with residue V3 and ends with residue L127 with one additional glycine derived from the construct. The final refinement statistics, native data, and phasing statistics are summarized in Supplementary Table 1. Figures were generated with the program Pymol (http://www.pymol.org/).

Enzyme linked immunosorbent assay (ELISA) for binding to RSV F protein

384-well plates were coated with 2 μg/mL of antigen overnight at 4 °C. Plates were blocked for with 2% milk supplemented with 2% goat serum for one hour, followed by three washes with PBS-T. Primary mAbs or B cell culture supernatants were applied to wells for two hours. Plates were washed with PBS-T four times before applying secondary antibody (goat anti-human IgG Fc, Meridian Life Science) at a dilution of 1:4,000 in blocking solution. After a one-hour incubation, the plates were washed six times with PBS-T, and phosphatase substrate solution (1 mg/mL phosphatase substrate in 1 M Tris aminomethane, Sigma) was added to each well. The plates were incubated at room temperature before reading the optical density at 405 nm on a Biotek plate reader.

Isolation of the 25P13 antibody

25P13 was isolated from the PBMCs of a Nashville Red Cross donor. PBMCs were isolated from human donor blood samples using Ficoll-Histopaque density gradient centrifugation. PBMCs were transformed with Epstein-Barr virus as described previously[34]. Cells were screened by ELISA for binding to post-fusion RSV F, and positive wells were fused with HMMA2.5 myeloma cells using the previously published protocol[34]. The 25P13 hybridoma was biologically cloned by single-cell fluorescence-activated sorting. The 25P13 hybridoma was expanded step-wise into 48-well and 12-well plates followed by 75-cm^2 flask in Media E (StemCell Technologies). Antibody production was accomplished by expanding the hybridoma to four 225-cm^2 cell culture flasks in serum-free medium (Hybridoma-SFM, GIBCO). After 21 days, supernatants were sterile filtered using 0.45 μm pore size filter devices. For antibody purification, HiTrap MabSelectSure columns (GE Healthcare Life Sciences) were used to purify antibodies using the manufacturer's protocol.

RSV and HMPV neutralization experiments

25P13 isolated from hybridoma supernatants were incubated 1:1 with a suspension of infectious RSV strain A2 for 1 hr. Following this, confluent HEp-2 cells, maintained in Opti-MEM I+GlutaMAX (Fisher) supplemented with 2% fetal bovine serum at 37 °C in a CO_2 incubator, in 24-well plates were inoculated with 50 μL of the antibody:virus mixture for one hr. After one hour, cells were overlaid with 1 mL of 0.75% methylcellulose dissolved in Opti-MEM I + GlutaMAX. Cells were incubated for four days after which the plaques were visualized by fixing cells with 10% neutral-buffered formalin and staining with crystal violet.

Neutralization experiments with hMPV used strain TN/96-12, which was obtained originally from a nasopharyngeal-wash specimen from a young child with upper respiratory tract illness in 1996 in Nashville, TN. Virus was grown in Vero cells with Opti-MEM I+ GlutaMAX medium (Fisher) 37 °C in a CO_2 incubator. The medium for cell propagation was supplemented with 2% fetal bovine serum. Confluent Vero cell monolayer cultures in 24-well plates were washed once with Opti-MEM I+GlutaMAX to remove serum, and then incubated with HMPV:mAb mixtures for one hour. Following this, the cells were overlaid with 0.75% methylcellulose in Opti-MEM I+GlutaMAX containing 5 μg/mL trypsin. Cells were incubated for four days before being fixed with neutral buffered formalin. Plaques were visualized by immunoperoxidase staining where anti-HMPV F guinea pig serum (or a mouse mAb targeting the HMPV nucleoprotein (Meridian Life Science) was used at 1:1,000 dilution in milk to overlay the cells for one hour, followed by incubation with 1:1,000 diluted goat anti-guinea pig IgG or anti-mouse IgG coupled to horseradish peroxidase (Meridian Life Science) for one hour. TrueBlue peroxidase substrate (Kirkegaard and Perry) then was added to visualize plaques. Plaques were counted and compared to the virus control. Data were analyzed with Prism software (GraphPad) to obtain IC_{50} values.

Competition binding

Competition binding was conducted on an OctetRed system (ForteBio) using anti-penta-HIS biosensors (ForteBio) and kinetics buffer (ForteBio). After obtaining an initial baseline in kinetics buffer, 10 μg/mL of his-tagged RSV F postfusion or prefusion (DSCAV1) protein

was immobilized onto anti-penta-HIS biosensor tips for 120 s. The baseline signal was measured again for 60 s before biosensor tips were immersed into wells containing 100 μg/mL primary antibody for 300 s. Following this, biosensors were immersed into wells containing 100 μg/mL of a second mAb for 300 s. Percent binding of a second mAbs in the presence of the first mAb was determined by comparing the maximal signal of the second mAb after the first mAb was added to the maximum signal of the second mAb alone. MAbs were considered non-competing if maximum binding of the second mAb was ≥ 66% of its un-competed binding. A level between 33%–66% of its uncompeted binding was considered intermediate competition, and ≤ 33% was considered competing.

Supplementary Material

Refer to Web version on PubMed Central for supplementary material.

Acknowledgments

We thank the members of the Jardetzky, Lamb and Crowe laboratories. This research was supported in part by National Institute of Health Research Grants AI-23173 (to R.A.L) and GM-61050 (to T.S.J). R.A.L. is an Investigator of the Howard Hughes Medical Institute.

J.E.C. is a consultant to Compuvax and a member of the Scientific Advisory Board of Meissa Vaccines.

References

1. Collins, PL., Crowe, JE, Jr. Fields Virology. Knipe, DM., Howley, PM., editors. Lippincott Williams & Wilkins; 2013.
2. Hall CB, Simoes EA, Anderson LJ. Clinical and epidemiologic features of respiratory syncytial virus. Curr Top Microbiol Immunol. 2013; 372:39–57. [PubMed: 24362683]
3. Falsey AR, Hennessey PA, Formica MA, Cox C, Walsh EE. Respiratory syncytial virus infection in elderly and high-risk adults. N Engl J Med. 2005; 352:1749–1759. [PubMed: 15858184]
4. Hall CB. The burgeoning burden of respiratory syncytial virus among children. Infectious disorders drug targets. 2012; 12:92–97. [PubMed: 22335498]
5. Edwards KM, et al. Burden of human metapneumovirus infection in young children. N Engl J Med. 2013; 368:633–643. [PubMed: 23406028]
6. Williams JV, et al. Human metapneumovirus and lower respiratory tract disease in otherwise healthy infants and children. N Engl J Med. 2004; 350:443–450. [PubMed: 14749452]
7. Fenton C, Scott LJ, Plosker GL. Palivizumab : A Review of its Use as Prophylaxis for Serious Respiratory Syncytial Virus Infection. Paediatr Drugs. 2004; 6:177–197. [PubMed: 15170364]
8. Palivizumab, a humanized respiratory syncytial virus monoclonal antibody, reduces hospitalization from respiratory syncytial virus infection in high-risk infants. The IMpact-RSV Study Group. Pediatrics. 1998; 102:531–537.
9. Bhattacharyya S, Gesteland PH, Korgenski K, Bjornstad ON, Adler FR. Cross-immunity between strains explains the dynamical pattern of paramyxoviruses. Proc Natl Acad Sci U S A. 2015; 112:13396–13400. [PubMed: 26460003]
10. Corti D, et al. Cross-neutralization of four paramyxoviruses by a human monoclonal antibody. Nature. 2013; 501:439–443. [PubMed: 23955151]
11. Schuster JE, et al. A broadly neutralizing human monoclonal antibody exhibits in vivo efficacy against both human metapneumovirus and respiratory syncytial virus. J Infect Dis. 2015; 211:216–225. [PubMed: 24864121]
12. Jardetzky TS, Lamb RA. Activation of paramyxovirus membrane fusion and virus entry. Curr Opin Virol. 2014; 5:24–33. [PubMed: 24530984]

13. Wen X, et al. Structure of the human metapneumovirus fusion protein with neutralizing antibody identifies a pneumovirus antigenic site. Nat Struct Mol Biol. 2012; 19:461–463. [PubMed: 22388735]
14. McLellan JS, et al. Structure of RSV fusion glycoprotein trimer bound to a prefusion-specific neutralizing antibody. Science. 2013; 340:1113–1117. [PubMed: 23618766]
15. McLellan JS, Yang Y, Graham BS, Kwong PD. Structure of the Respiratory Syncytial Virus Fusion Glycoprotein in the Post-fusion Conformation Reveals Preservation of Neutralizing Epitopes. J Virol. 2011; 85:7788–7796. doi:JVI.00555-11[pii]10.1128/JVI.00555-11. [PubMed: 21613394]
16. Swanson KA, et al. Structural basis for immunization with postfusion respiratory syncytial virus fusion F glycoprotein (RSV F) to elicit high neutralizing antibody titers. Proc Natl Acad Sci U S A. 2011; 108:9619–9624. doi:1106536108[pii]10.1073/pnas.1106536108. [PubMed: 21586636]
17. Yin HS, Wen X, Paterson RG, Lamb RA, Jardetzky TS. Structure of the parainfluenza virus 5 F protein in its metastable, prefusion conformation. Nature. 2006; 439:38–44. [PubMed: 16397490]
18. Mas V, et al. Engineering, Structure and Immunogenicity of the Human Metapneumovirus F Protein in the Postfusion Conformation. PLoS Pathog. 2016; 12:e1005859. [PubMed: 27611367]
19. Joyce MG, et al. Iterative structure-based improvement of a fusion-glycoprotein vaccine against RSV. Nat Struct Mol Biol. 2016
20. Boyington JC, et al. Structure-Based Design of Head-Only Fusion Glycoprotein Immunogens for Respiratory Syncytial Virus. PLoS One. 2016; 11:e0159709. [PubMed: 27463224]
21. Stewart-Jones GB, et al. A Cysteine Zipper Stabilizes a Pre-Fusion F Glycoprotein Vaccine for Respiratory Syncytial Virus. PLoS One. 2015; 10:e0128779. [PubMed: 26098893]
22. McLellan JS, et al. Structure-based design of a fusion glycoprotein vaccine for respiratory syncytial virus. Science. 2013; 342:592–598. [PubMed: 24179220]
23. Wen X, et al. A Chimeric Pneumovirus Fusion Protein Carrying Neutralizing Epitopes of Both MPV and RSV. PLoS One. 2016; 11:e0155917. [PubMed: 27224013]
24. Gilman MS, et al. Characterization of a Prefusion-Specific Antibody That Recognizes a Quaternary, Cleavage-Dependent Epitope on the RSV Fusion Glycoprotein. PLoS Pathog. 2015; 11:e1005035. [PubMed: 26161532]
25. Lee PS, Wilson IA. Structural characterization of viral epitopes recognized by broadly cross-reactive antibodies. Curr Top Microbiol Immunol. 2015; 386:323–341. [PubMed: 25037260]
26. Doria-Rose NA, Joyce MG. Strategies to guide the antibody affinity maturation process. Curr Opin Virol. 2015; 11:137–147. [PubMed: 25913818]
27. Schmidt AG, et al. Viral receptor-binding site antibodies with diverse germline origins. Cell. 2015; 161:1026–1034. [PubMed: 25959776]
28. Zhou T, et al. Structural Repertoire of HIV-1-Neutralizing Antibodies Targeting the CD4 Supersite in 14 Donors. Cell. 2015; 161:1280–1292. [PubMed: 26004070]
29. Storoni LC, McCoy AJ, Read RJ. Likelihood-enhanced fast rotation functions. Acta Crystallogr D Biol Crystallogr. 2004; 60:432–438. [PubMed: 14993666]
30. Collaborative Computational Project, N. The CCP4 suite: programs for protein crystallography. Acta Crystallogr D Biol Crystallogr. 1994; 50:760–763. [PubMed: 15299374]
31. Zwart PH, et al. Automated structure solution with the PHENIX suite. Methods Mol Biol. 2008; 426:419–435. [PubMed: 18542881]
32. Adams PD, et al. PHENIX: building new software for automated crystallographic structure determination. Acta Crystallogr D Biol Crystallogr. 2002; 58:1948–1954. [PubMed: 12393927]
33. Emsley P, Cowtan K. Coot: model-building tools for molecular graphics. Acta Crystallogr D Biol Crystallogr. 2004; 60:2126–2132. [PubMed: 15572765]
34. Smith SA. Persistence of circulating memory B cell clones with potential for dengue virus disease enhancement for decades following infection. J Virol. 2012; 86:2665–2675. [PubMed: 22171265]

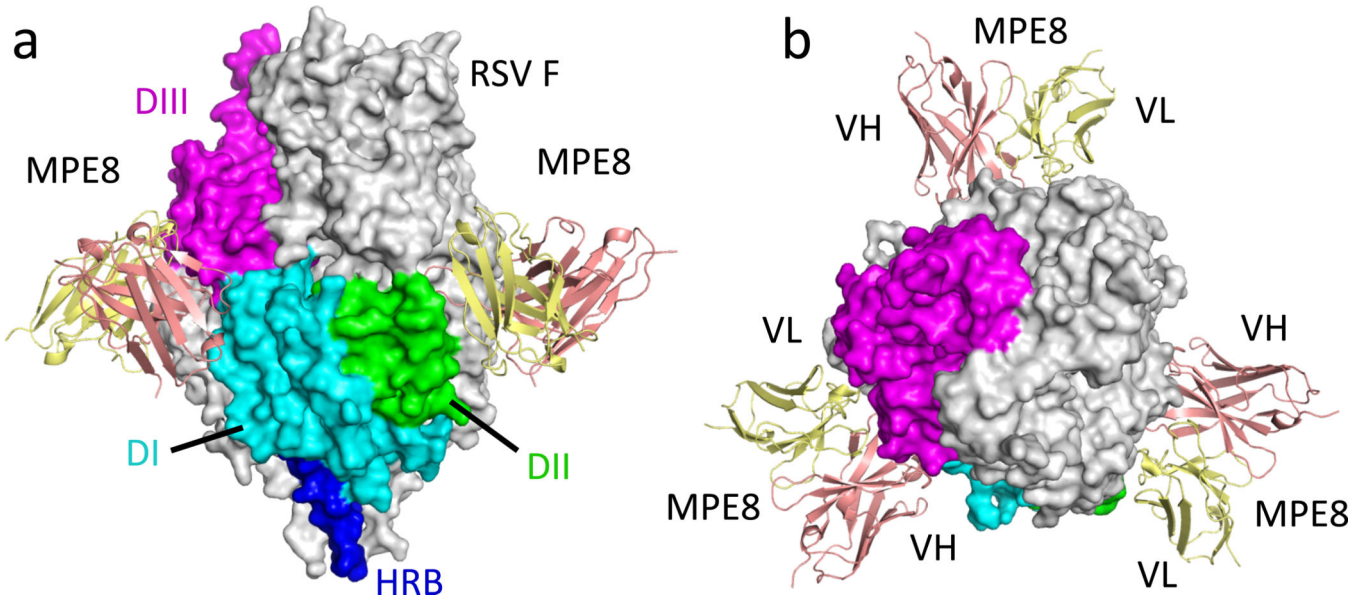

Fig. 1. Overall structure of the RSV F:MPE8 complex

(a,b) Structure of the complex of MPE8 scFv with prefusion RSV F. RSV F subunits are shown in surface format. Two subunits are colored light grey. The third subunit is colored by domain (DI: cyan; DII: green; DIII: magenta: heptad repeat B (HRB): blue). The MPE8 scFvs are shown in cartoon format with VH colored salmon and VL colored yellow. The view in (b) is rotated 90° from (a) and oriented down the 3-fold axis of the F trimer. MPE8 binds an epitope in the midsection of the RSV F ectodomain at the intersection of DI, DII and DIII domains from two subunits of the F trimer.

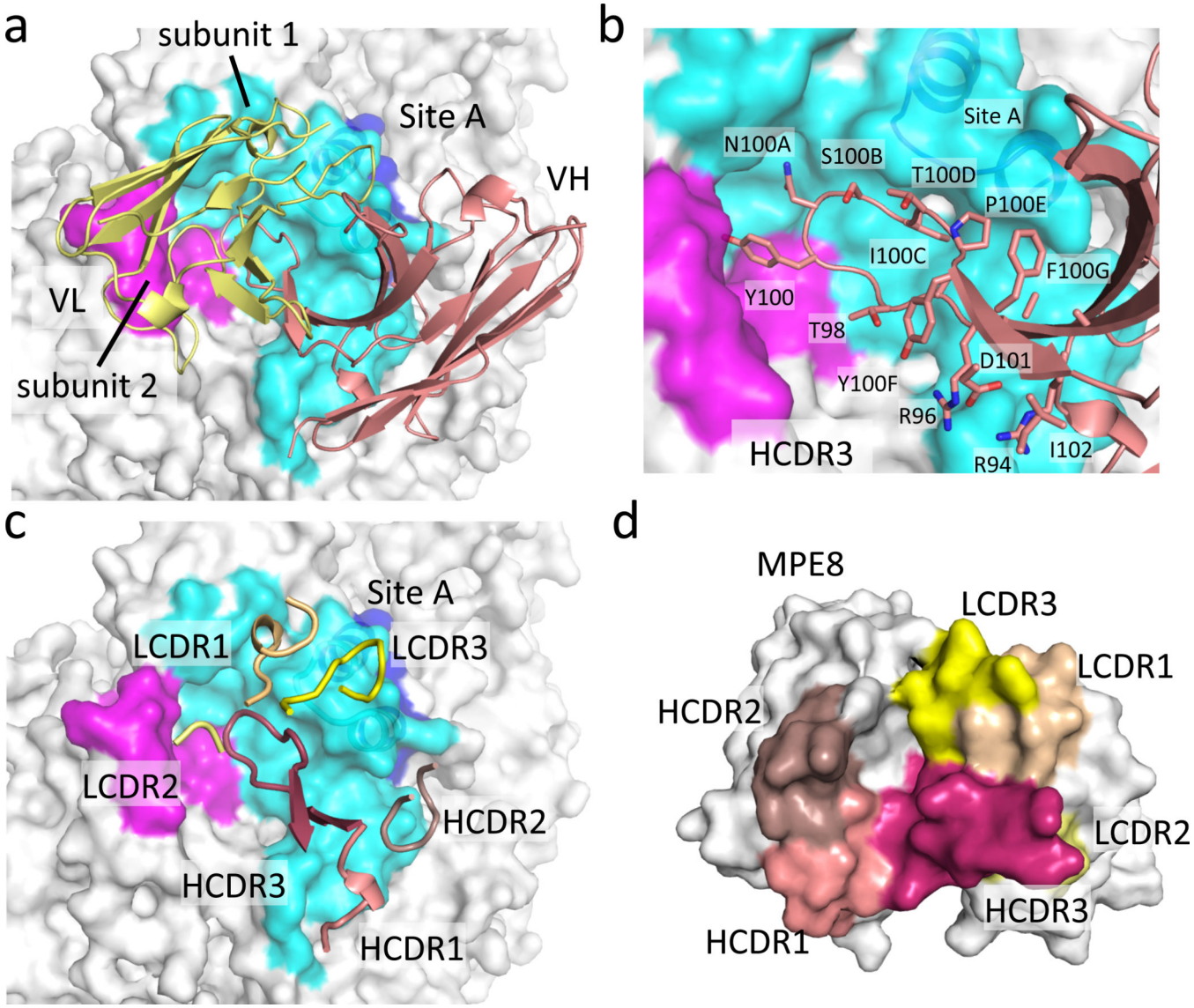

Fig. 2. The MPE8 epitope and paratope

(a) The MPE8 epitope is formed by residues from two adjacent F subunits. MPE8 is shown in cartoon format, with VH in pink and VL in yellow. The RSV F surface is shown, with interacting residues colored cyan and magenta in the two subunits as indicated. (b) HCDR3 extends into a deep pocket at the F intersubunit interface, making contacts with both chains that are dependent on the prefusion F conformation. The HCDR3 extends underneath the Site A helix-turn-helix motif recognized by palivizumab/motavizumab. (c) MPE8 CDR loops form an extensive interface with RSV F, with HCDR1, HCDR2, LCDR1 and LCDR3 contacting one subunit. LCDR2 contacts a second subunit of F, while HCDR3 interacts with both. LCDR1 interacts with beta strands in HRA that refold to helices in the postfusion conformation. (d) HCDR3 folds over the surface of the VH and VL interface, covering residues of LCDR2 implicated in crossreactive recognition of RSV and HMPV F.

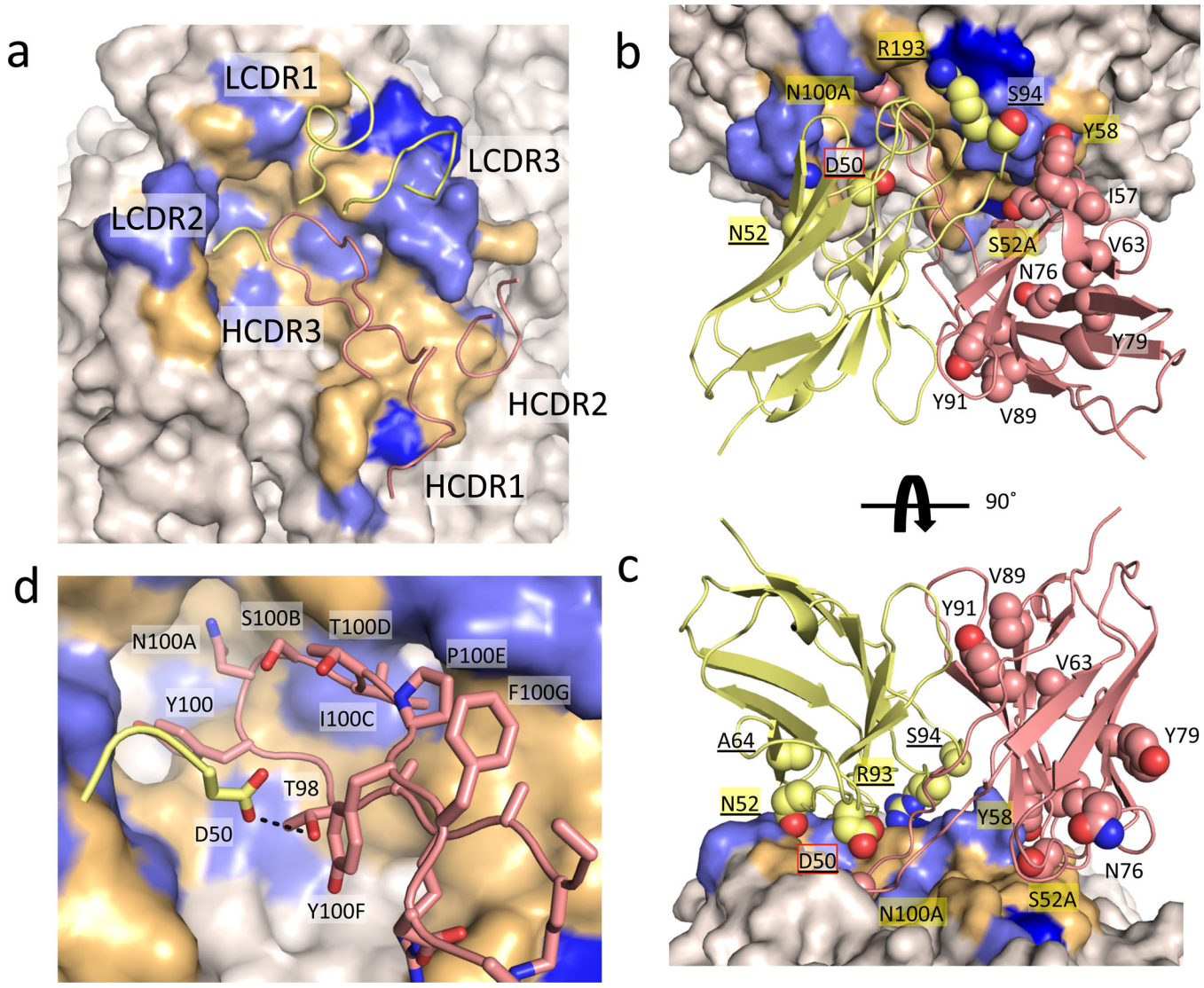

Fig. 3. Structural basis for MPE8 cross-reactivity

(a) HCDR1, HCDR2 and HCDR3 interact with a contiguous patch of conserved residues within the MPE8 epitope on F. The RSV F epitope is colored by conservation (conserved: light orange; not conserved between RSV/HMPV: medium blue; not conserved between HMPV A/B strains: dark blue) (b) Location of predicted somatic mutations in mature MPE8.. Somatically mutated residues are shown as spheres. Residue labels with yellow background indicate residues forming contacts with RSV F. The label for LCDR2 residue D50 is highlighted with a red box. MPE8 VH and VL are shown in cartoon format, colored pink and yellow, respectively. The view in panel (c) is rotated 90° about the horizontal from panel (b). (d) VL D50 within LCDR2 does not directly contact RSV F. D50 makes a hydrogen bond to the sidechain of HCDR3 residue T98, which could impact HCDR3 conformation and HMPV cross-reactivity.

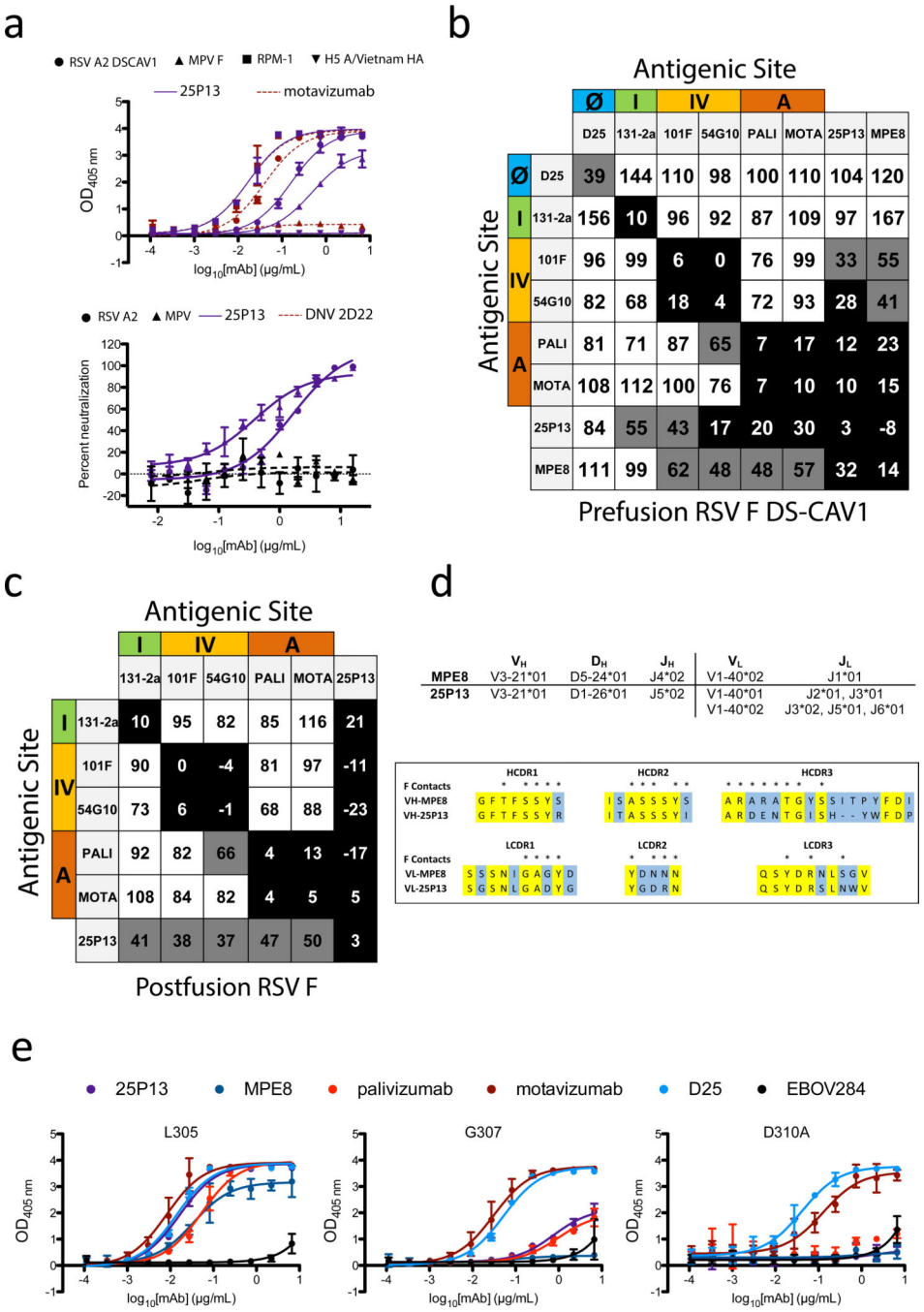

Fig. 4. 25P13 is an MPE8-related cross-reactive neutralizing antibody

(a) 25P13 binds both RSV and HMPV F proteins and neutralizes both viruses. (b) Epitope binning using the OctetRed system with anti-penta-HIS biosensors. Sensors were coated with RSV A2 fusion protein (DS-Cav1, prefusion conformation). Horizontal mAbs were loaded first, followed by the vertical mAbs. MAbs were judged to compete for the same site if maximum binding of the competing mAb was reduced to <33% of its un-competed binding (black boxes with white numbers). MAbs were considered non-competing if maximum binding of the competing mAb was >66% of its un-competed binding (white

boxes with red numbers). Gray boxes with black numbers indicate an intermediate phenotype (between 33 and 66% of un-competed binding). (c) Epitope binning using OctetRed system with anti-penta-HIS biosensors. Sensors were coated with RSV A2 fusion protein (postfusion conformation, fusion peptide removed). Horizontal mAbs were loaded first, followed by the vertical mAbs. MAbs were judged to compete for the same site if maximum binding of the competing mAb was reduced to <33% of its un-competed binding (black boxes with white numbers). MAbs were considered non-competing if maximum binding of the competing mAb was >66% of its un-competed binding (white boxes with red numbers). Gray boxes with black numbers indicate an intermediate phenotype (between 33 and 66% of un-competed binding). (d) 25P13 uses the same VH and VL segments as MPE8 and shows homology in the HCDR3 and LCDR3 sequences. Many conserved amino acids of the 25P13 LCDR3 correspond to the F-contacting residues in MPE8 (indicated above the sequences), suggesting a similar mode of F engagement. (e) Antibody ELISA assays with RSV F mutants that disrupt MPE8 binding[10] and lie within the MPE8 epitope (D310A and G307R).